TITLE: Functional variations in gamma-secretase activity are critical determinants of the clinical, biomarker, and cognitive progression of autosomal dominant Alzheimer's disease

AUTHOR LIST Stephanie A. Schultz, PhD[1], Lei Liu, MD, PhD[2,3], Aaron P. Schultz, PhD[1], Colleen D. Fitzpatrick, MA[1], Raina Levin, BS[1], Jean-Pierre Bellier, PhD[2,3], Zahra Shirzadi, PhD[2,3], Nelly Joseph-Mathurin, PhD[4], Charles D. Chen, PhD[4], Tammie L.S. Benzinger, MD, PhD[4], Gregory S. Day, MD[5], Martin R. Farlow, MD[6], Brian A. Gordon, PhD[4], Jason J. Hassenstab, PhD[4], Clifford R. Jack Jr., MD[7], Mathias Jucker, PhD[8], Celeste M. Karch, PhD[4], Jae-Hong Lee, MD, PhD[9], Johannes Levin, MD[10-12], Richard J. Perrin, MD, PhD[4], Peter R Schofield, PhD, DSc[13,14], Chengjie Xiong, PhD[4], Keith A. Johnson, MD[1,2], Eric McDade, DO[4], Randall J. Bateman, MD[4], Reisa A. Sperling, MD[1,2], Dennis J. Selkoe, MD[2,3], Jasmeer P. Chhatwal, MD, PhD, MMSc*[1,2,3], and the Dominantly Inherited Alzheimer Network Investigators

[1]Massachusetts General Hospital, Harvard Medical School; Boston, MA, USA

[2]Brigham and Women's Hospital; Boston, MA, USA

[3]Ann Romney Center for Neurologic Diseases; Boston, MA, USA

[4]Washington University in St. Louis School of Medicine; St. Louis, MO, USA

[5]Mayo Clinic; Jacksonville, FL, USA

[6]Indiana Alzheimer's Disease Research Center; Indianapolis, IN, USA

[7]Mayo Clinic, Rochester; MN, USA

[8]German Center for Neurodegenerative Diseases (DZNE); Tuebingen, Germany

[9]Asan Medical Center, University of Ulsan College of Medicine; Seoul, Korea

[10]German Center for Neurodegenerative Diseases (DZNE); Munich, Germany

[11]Department of Neurology, Ludwig-Maximilians-Universität München; Munich, Germany

[12]Munich Cluster for Systems Neurology (SyNergy); Munich, Germany

[13]Neuroscience Research Australia; Randwick, NSW, Australia

[14]School of Medical Sciences, University of New South Wales; Sydney, NSW, Australia

*Corresponding author: Jasmeer P. Chhatwal MD, PhD, MMSc; Email: Chhatwal.Jasmeer@mgh.harvard.edu

ABSTRACT

Background: The balance between production, clearance, and toxicity of Aβ peptides is central to Alzheimer's disease (AD) pathobiology. Though highly variable in terms of age at symptom onset (AAO), hundreds of variants in *PSEN1* cause autosomal dominant forms of AD (ADAD) with nearly complete penetrance. PSEN1 forms the catalytic core of the γ-secretase complex and thereby directly mediates the production of longer, aggregation-prone Aβ peptides relative to shorter, non-aggregating peptides. We hypothesized that the broad AAO and biomarker heterogeneity seen across ADAD would be predictable based on mutation-specific differences in the production of Aβ species.

Methods: Aβ-37, 38, 40, 42, and 43 production was quantified from 161 unique *PSEN1* variants expressed in HEK293 cells. Prediction of AAO was carried out in 106 variants with available AAO and then replicated in 55 variants represented across 190 PSEN1 mutation carriers who have detailed cognitive and biomarker data from the Dominantly Inherited Alzheimer's Network (DIAN).

Results: Variations in Aβ production across the 161 mutations examined in cell-based models were highly predictive of AAO. In those with corresponding *in vivo* data from the DIAN study, our cell-based γ-secretase composite was strongly associated with biomarker and cognitive trajectories.

Conclusions: These findings elucidate the critical link between γ-secretase function, Aβ production, and AD progression and offer mechanistic support for the amyloid hypothesis. The approach used here represents a powerful tool to account for heterogeneity in disease progression in ADAD clinical trials and to assess the pathogenicity of variants of unknown significance or with limited family history.

INTRODUCTION

An increase in longer, aggregation-prone Aβ fragments (e.g., Aβ 42 and 43) relative to shorter, non-aggregating fragments (e.g., Aβ 37 and 38) is a critical initiating pathogenic event in both late-onset, sporadic AD[1] (LOAD) and Autosomal Dominant AD[2–4] (ADAD). The balance between production of aggregating and non-aggregating forms of Aβ is a direct result of the efficiency and kinetics with which the γ-secretase proteolytic complex sequentially cleaves β-amyloid precursor protein[5–10] (APP). Subtle alterations in γ-secretase function can lead to profound neurodegenerative and cognitive consequences, while modulation of γ-secretase has therapeutic potential in both LOAD and ADAD[8,9,11–13]. Over 200 pathogenic variants in *Presenilin-1* (*PSEN1*), the key catalytic subunit in the γ-secretase complex, have been identified and are the most common causes of ADAD[14]. Mirroring the heterogeneity in clinical and AD biomarker progression seen in LOAD, there is striking heterogeneity in age of symptom onset (AAO)[15–17] and rates of cognitive and biomarker change[18–22] across carriers of *PSEN1* pathogenic variants. We hypothesized that this heterogeneity may be strongly tied to underlying mutation-level variation in γ-secretase function.

Intriguingly, prior work suggests some pathogenic *PSEN1* variants may not significantly alter the absolute amounts of Aβ42 production[23,24], indicating that more thorough investigation is needed to understand how these pathogenic variants lead to ADAD and the mechanisms that cause earlier vs. later disease onset and progression. To this end, findings from our group[25] and others[26] suggest that probing the ratios of short-to-long Aβ peptide production across ADAD pathogenic variants may help us understand the observed heterogeneity in these populations. However, this initial work

98 examined only a small number of variants, used only AAO information derived from the
99 literature, and lacked biomarker, clinical, and cognitive data.

100 Here, we leverage a live-cell-based model system and newly developed
101 immunoassays to functionally characterize APP processing by γ-secretase across a
102 large set of *PSEN1* pathogenic variants with AAOs ranging from the 20s to the 70s. We
103 then assess how this mutation-level characterization of γ-secretase function may
104 explain heterogeneity in neuroimaging and biofluid biomarkers, as well as clinical
105 measures among *PSEN1* carriers with available data from the Dominantly Inherited
106 Alzheimer's Network Observational Study (DIAN-Obs).

107

108 **METHODS**

109 **Functional assays of γ-secretase function**

110 161 unique *PSEN1* variants, including 55 unique variants represented in DIAN-Obs and
111 data from 106 unique variants previously characterized in Liu et al., 2022,[25] and wild-
112 type (normal) *PSEN1* was characterized for Aβ peptide production and γ-secretase
113 function. Using methods detailed in supplemental methods and a prior report using this
114 model system, each *PSEN1* variant or normal *PSEN1* was sub-cloned and placed into
115 the PcDNA 3.1 expression vector[25]. Subsequently, each variant was co-transfected with
116 a plasmid encoding wild-type (normal) human APP-C99 into HEK293T cells genetically
117 depleted of *PSEN1* and *PSEN2*[25]. Creation of this cell line and transient transfection
118 procedures are described in supplemental methods. Conditioned media from
119 transfected HEK cells was harvested and diluted with 1% BSA in wash buffer (TBS
120 supplemented with 0.05% Tween). Aβ37, 38, 40, 42, and 43 immunoassays were

121 performed in triplicate and averaged as previously described[25] (see Figure S1 and
122 supplemental methods). Absolute peptide production levels and relevant ratios were
123 examined as percent relative to the production seen in the same model system
124 following transfection with normal (wild-type) *PSEN1.*
125
126 **Participants**
127 Participants provided written informed consent prior to the completion of any study
128 procedures, in accordance with Institution Review Board policy at each participating
129 site. Data were included from 190 *PSEN1* pathogenic variant carriers enrolled in DIAN-
130 Obs, each carrying one of 55 unique *PSEN1* pathogenic variants characterized via cell-
131 based methods (see Figure 1A, Table S1, and Table S2). Detailed protocols for DIAN
132 have previously been published and are described in supplemental methods. For DIAN-
133 Obs participants, the familial AAO was determined through structured interviews to
134 determine the age of onset of progressive cognitive decline for the participant's first
135 degree relative(s)[16].
136 Clinical evaluators were blind to the mutation status of participants. Participants
137 underwent comprehensive clinical and cognitive evaluations. Clinical Dementia Rating
138 (CDR®) Sum of Boxes (SB) was assessed for each participant using structured
139 interviews, as previously described[27]. Mini-Mental State Examination (MMSE) and
140 Wechsler Memory Scale-Revised Logical Memory Delayed Recall[28] were selected a
141 priori as our cognitive measures of interest. All DIAN-Obs participants with available Aβ
142 positron emission tomography (PET), magnetic resonance imaging (MRI), and at least
143 one cognitive assessment were included (Figure 1A; DIAN-Obs data freeze version 15;

144 last data from June 30, 2020; see supplemental methods). A subset of these individuals
145 also had [^{18}F]Fluorodeoxyglucose (FDG)-PET (n=162) and cerebrospinal fluid (CSF)
146 (n=157) available for analyses. Longitudinal data were available from 154 DIAN
147 participants (Table S3). For the 106 *PSEN1* variants studies previously in Liu et al.
148 (non-overlapping with the 55 variants from DIAN-Obs), AAO was derived from prior
149 literature, as previously described[25].
150

151 **Imaging and Fluid Biomarker Analyses**

152 Protocols for Aβ and brain metabolism PET, MRI, and CSF studies are described in
153 detail in supplemental methods and in previously published work[22,27,29–33]. Cerebral Aβ
154 load was measured using [^{11}C]Pittsburgh Compound B (PiB) PET, and brain glucose
155 metabolism was measured with [^{18}F]FDG-PET. Partial volume corrected values were
156 used in all analyses. FreeSurfer v 5.3 defined regional measures were derived from MRI
157 data. CSF Aβ42, Aβ40, and phosphorylated-tau181 levels were measured using an
158 automated immunoassay system (LUMIPULSE G1200, Fujirebio, Malvern, PA).
159 Phosphorylated-tau 217 (pT217/T217) values were derived from immunoprecipitation-
160 mass spectrometry (IP-MS) as previously described[29]. See supplemental methods for
161 additional details.
162

163 **Statistical Analyses**

164 Analyses were conducted using R (version 4.0.3, R Foundation for Statistical
165 Computing). Pearson correlations were used to assess associations of Aβ production
166 and γ-secretase function with AAO. A summary measure of variant-level Aβ production

167 and γ-secretase function (γ-secretase composite) was developed to reduce the number
168 of statistical comparisons and facilitate comparisons between mutant and wild-type
169 *PSEN1*, as described in the Results.

170 Linear mixed effect models including fixed effects for age, sex, and γ-secretase
171 composite score were employed to assess associations between the cell-based γ-
172 secretase function and multi-modal biomarker and clinical data from DIAN. Similar to
173 prior work from DIAN, a random effect for family membership was included in each
174 linear mixed effects model. Separate models were used to assess associations with
175 each clinical, cognitive, or biomarker outcome measure, focusing on CSF Aβ 42/40,
176 CSF phosphorylated-tau 181, CSF phosphorylated-tau 217, hippocampal volume, CDR-
177 SB, MMSE, and logical memory delayed (see supplemental methods). Years of
178 education was included as an additional fixed effect term in models examining cognitive
179 and clinical outcomes. Longitudinal models were similarly constructed but additionally
180 included interactions of each fixed effect with time and terms allowing both a random
181 intercept and slope. Additional exploratory analyses made use of a tertile split of γ-
182 secretase composite scores to visualize how clinical, cognitive, and biomarker
183 trajectories can be understood in the context of γ-secretase function.
184

185 **RESULTS**
186

187 **Cell-based measures of γ-secretase function are associated with age of symptom**
188 **onset.**

189 Aβ 37, 38, 40, 42, and 43 production was assessed in 161 unique *PSEN1* variants,
190 including 55 *PSEN1* variants represented in DIAN (Table S1) and 106 non-overlapping

variants previously characterized in Liu et al., 2022[25]. Grouping together Aβ production for all 161 variants, we observed reductions in Aβ37, 38, and 40 compared to normal levels (median % reduction relative to normal = -56.8, -48.6, and -22.8%, respectively), suggesting that, as a group, *PSEN1* pathogenic variants decrease the processive γ-cleavage of Aβ by γ-secretase (γ-processivity), leading to a decrease in these fully processed (shorter) Aβ peptides. Additionally, relative levels of Aβ42 and 43 across variants were higher in *PSEN1* pathogenic variants compared to normal levels (median % increase relative to normal= 66.5% and 47.1%; respectively).

We first assessed relationships between the relative concentrations of Aβ species produced by each variant and AAO in a set of 106 variants not represented in the DIAN study. To limit comparisons with multiple ratios when assessing relationships between γ-secretase function and AAO, we leveraged prior literature[1,25,26,34,35] suggesting the Aβ 42/40 ratio and a measure of the efficiency of successive cleavage (γ-processivity) of Aβ fragments can be used to summarize γ-secretase function. These two measures were operationalized as $\log_{10}(\frac{\text{A}\beta42}{\text{A}\beta40})$ (a measure of the relative production of aggregation-prone Aβ) and a ratio of short (fully γ-secretase processed) to long (incompletely γ-secretase processed) Aβ fragments ($\frac{\text{short A}\beta37+38}{\text{long A}\beta42+43}$). As expected, $\frac{\text{A}\beta42}{\text{A}\beta40}$, and $\frac{\text{short A}\beta37+38}{\text{long A}\beta42+43}$ ratio levels across *PSEN1* pathogenic variants were both abnormal (decreased processivity) compared to normal levels (median % change relative to the normal = 108.9 and -71.3%). In the initial sample of 106 *PSEN1* pathogenic variants from Liu et al., both higher $\log_{10}(\frac{\text{A}\beta42}{\text{A}\beta40})$ (r[105] = -0.64, p = 2.20e-13) and lower

212 $\frac{\text{short A}\beta37+38}{\text{long A}\beta42+43}$ (r[105] = 0.66, p =2.28e-14) levels were associated with earlier AAO (Figure
213 1B-C). Both ratios remained significantly associated when entered together into a single
214 model predicting AAO (Table S4), suggesting that they capture unique variance with
215 respect to the pathogenicity of each variant. Accordingly, these two ratios were
216 combined into a single summary measure of variant-level γ-secretase function (γ –
217 secretase $Composite = \frac{short\ A\beta37+38}{long\ A\beta42+43} - log_{10}\frac{A\beta42}{A\beta40}$). To facilitate visualization and
218 comparison, the γ-secretase composite is expressed as a percentage of wild-type γ-
219 secretase function.

220 In both the subset of variants represented in the DIAN-Obs and remaining
221 variants characterized previously by Liu et al[25], γ-secretase composite scores were
222 lower in all pathogenic variants compared to normal (average of 60.4% reduction
223 relative to normal). The γ-secretase composite had a the highest degree of correlation
224 with AAO (Liu et al cohort: r[105] = 0.71, p <2.2e-16; DIAN-Obs cohort: r[53] = 0.61, p =
225 6.10e-07; Figure 1E), as compared to using individual Aβ peptide levels, $\frac{\text{A}\beta42}{\text{A}\beta40}$ levels, or
226 $\frac{\text{short A}\beta37+38}{\text{long A}\beta42+43}$ ratio levels in the initial set of 106 *PSEN1* variants and in the 55 variants
227 represented in DIAN (see above). To demonstrate the potential utility of using the γ-
228 secretase composite to predict an approximate AAO for novel pathogenic variants
229 and/or when a clinical history is not available, we list the γ-secretase composite derived
230 AAO (AAO_{gsc}) values for the variants examined here (Table S1). Notably, γ-secretase
231 composite values did not map in a straightforward manner onto the location of the
232 corresponding pathogenic variant within *PSEN1*, and substantial variation within a

233 single codon in terms of γ-secretase function was observed for several sites in which
234 more than one variant was characterized (Table S1; Figure 1D).
235
236 **Lower cell-based γ-secretase composite scores are associated with more**
237 **abnormal AD imaging and fluid biomarkers.**
238 Lower γ-secretase composite scores (decreased γ-secretase function relative to
239 normal) were associated with higher levels of mean cortical Aβ burden (B[SE] = -
240 0.03[0.01], p =4.06e-07; Figure 2A) as assessed by Aβ PET, after controlling for
241 demographic factors. Exploratory regional analyses revealed widespread associations
242 between *in vivo* Aβ burden and the cell-based γ-secretase composite, with the strongest
243 associations seen in the precuneus, and anterior and posterior cingulate (Figure 2D).
244 We next examined associations between the variant-level γ-secretase composite
245 and commonly used imaging biomarkers of neurodegeneration, including structural MRI
246 and FDG-PET, in DIAN-Obs participants carrying one of the 55 of the *PSEN1* variants
247 characterized *in vitro*. Both the MRI-based measures hippocampal volume (B[SE] =
248 44.22[6.4], p = 5.15e-10; Figure 2B) and precuneus FDG-PET signal (B[SE] =
249 0.006[0.001], p = 5.38e-05; Figure 2C) were highly associated with the γ-secretase
250 composite, after controlling for demographic factors. Exploratory regional analyses
251 revealed that the cell-based γ-secretase composite significantly accounted for
252 widespread grey matter volume differences across *PSEN1* variant carriers, most
253 notably in the hippocampus, amygdala, temporal regions, precuneus, and posterior
254 cingulate (Figure 2E), as well as differences in glucose metabolism including the
255 precuneus, parietal, and frontal regions (Figure 2F).

256 Using established CSF measures of AD pathology, we observed that lower
257 variant-specific γ-secretase composite scores were associated with lower CSF Aβ 42/40
258 (B[SE] = 6.3e-04[1.5e-04], p = 4.46e-05; Figure 3A), higher CSF ELISA
259 $\log_{10}$(phosphorylated-tauT181) levels (B[SE] = -0.009[0.002], p =4.47e-06; Figure 3B),
260 and higher CSF IP-MS $\log_{10}$(pT217/T217) levels (B[SE] = -0.01[0.002], p =1.98e-05;
261 Figure 3C).
262
263 **γ-secretase composite scores are associated with clinical and cognitive measures**
264 **in *PSEN1* pathogenic variant carriers in DIAN-Obs.**
265 The cell-derived γ-secretase composite levels predicted changes of MMSE
266 (B[SE] = 0.11[.03], p = 2.17e-04; Figure 3D), CDR-SB (B[SE] = -0.07[0.02], p = 4.86e-
267 05; Figure 3E), and logical memory-delayed scores (B[SE] = 0.11[.03], p = 6.51e-05;
268 Figure 3F).
269
270 **γ-secretase composite scores predict rate of change in biomarker, clinical and**
271 **cognitive features in *PSEN1* ADAD carriers.**
272 We next assessed how longitudinal rates of change in core biomarker, clinical,
273 and cognitive measures of interest (Figure 4A, C, E, and G) may be related to cell-
274 based measures of γ-secretase function. Lower (more pathogenic) γ-secretase
275 composite measures were associated with faster increase in β-amyloid PET signal
276 (B[SE] = -7.2e-04[2e-04], p = 0.003; Figure 4B), as well as more rapid decreases in
277 hippocampal volume (B[SE] = 4.56[0.7], p = 2.96e-10; Figure 4D), MMSE (B[SE] =

278 0.02[0.007], p = 3.02e-04; Figure 4F), and logical memory-delayed (B[SE] =
279 0.006[0.001], p = 2.63e-06; Figure 4H).
280
281 **Multimodal models suggest variant level variations in γ-secretase function may**
282 **impact the clinical, cognitive, and biomarker progression of ADAD.**
283 To assess how differences in γ-secretase function may alter the observed
284 clinical, cognitive, and biomarker course of ADAD, we performed a tertile split of
285 variants represented in DIAN and plotted the standardized change in core clinical,
286 cognitive, and biomarker measures across the lifespan for individuals carrying *PSEN1*
287 pathogenic mutations in the lowest, middle, or highest tertile of γ-secretase function
288 (Figure 5A-C). To complement this group-level analysis, we used all available data to
289 visualize putative disease trajectories for carriers of 2 hypothetical variants with 25%
290 and 75% of normal γ-secretase function, respectively (Figure 5D-I). Consistent with the
291 foregoing analyses, these visualizations demonstrate an earlier shift in AAO, clinical and
292 biomarker abnormalities in carriers of variants with lower (more pathogenic) γ-secretase
293 composite scores. A similar pattern was seen when using estimated years to symptom
294 onset (EYO; calculated by subtracting history-derived AAO from the participant's age)
295 rather than age (Figure S2A-B). This suggests that cell-based assessments of γ-
296 secretase add to the prediction of disease trajectories even after history-derived
297 information about AAO is included in statistical models. However, while a shift in the
298 timing of symptom and biomarker changes was seen across a range of γ-secretase
299 function, it is notable that elevations in pathological Aβ burden (higher Aβ PET or lower
300 CSF Aβ42) and tau (higher CSF phosphorylated-tau181) appear to be early events

301 across all tertiles and precede changes in neurodegenerative markers (hippocampal
302 volume, FDG PET) and clinical measures of impairment (CDR-SB). Together, these
303 results suggest that, while mutation-level variations in γ-secretase function may impact
304 the age of symptom onset and rate of ADAD progression, the ordering of clinical,
305 cognitive, and biomarker changes is not itself fundamentally altered by differences in γ-
306 secretase function.
307
308 **DISCUSSION:**
309 The study of ADAD forms a cornerstone for understanding AD pathobiology, informing
310 the development of new AD biomarkers, broadly influencing the design of animal
311 models of AD, and advancing therapeutic approaches for both LOAD and ADAD. While
312 ADAD-causing *PSEN1* pathogenic variants are highly penetrant, remarkable
313 heterogeneity in the AAO, rates of disease progression, and biomarker changes is seen
314 across variants. Here we examined whether variant level differences in γ-secretase
315 processing of APP may be critical determinants of the age at which *PSEN1* pathogenic
316 variant carriers manifest cognitive changes and develop abnormalities in core
317 biomarkers for AD. Using a cell-based model system to assess the production of a
318 broad set of Aβ peptides, we observed that mutation level differences in γ-secretase
319 processing of APP strongly predicted the age at which progressive cognitive symptoms
320 are manifest (AAO) for a given variant. In addition to predicting AAO, we observed that
321 a summary measure of γ-secretase function was associated with the rates of functional
322 (CDR-SB) and cognitive decline. This composite measure of γ-secretase function was
323 also associated with all fluid and imaging biomarker measures of AD pathobiology and

324 neurodegeneration we examined, including CSF measures of AD pathology, Aβ PET,
325 FDG-PET, and MRI gray matter volumes. These results suggest that accounting for
326 mutation-level γ-secretase dysfunction may clarify treatment effects in ADAD clinical
327 trials and may also be useful in predicting approximate AAO and disease trajectories for
328 *PSEN1* pathogenic variants that are novel or lack sufficient clinical history.
329 Mechanistically, these results highlight the direct importance of γ-secretase function to
330 AD pathobiology and provide support for γ-secretase modulation as a potentially
331 powerful AD therapeutic and preventative strategy[36].

332 Using a human cell-based model system, we found substantial variability in the
333 production of shorter (Aβ-37 and 38) to longer (Aβ-42 and 43) Aβ peptides across
334 *PSEN1* pathogenic variants. The high-throughput nature of our human-cell-based
335 system enabled characterization of a large amount of *PSEN1* variants allowing a more
336 thorough comparison with AAO compared to what has been assessed precviously[26],
337 which in turn improves the generalizability of our findings with respect to autosomal
338 dominant Alzheimer's disease. In this same system, we observed that the Aβ42/40
339 ratio was increased in a majority but not all variants examined. We first examined 106
340 *PSEN1* variants with available AAO but no available clinical and biomarker data and
341 observed that both the ratio of short-to-long Aβ peptide production ($\frac{A\beta 37+38}{A\beta 42+43}$) and the
342 more commonly used Aβ 42/40 ratio were predictive of AAO. These results in PSEN1
343 variants without biomarker, cognitive, and clinical data are concordant with the recent
344 findings in a much small number of *PSEN1* variants from Petit and colleagues[26], a study
345 which used virally induced mouse embryonic fibroblasts as a model system.
346

347 Intriguingly, the short-to-long and Aβ 42/40 ratios were independently associated
348 with AAO, and a composite measure derived from these two ratios provided stronger
349 associations with AAO than either alone. This composite measure was carried forward
350 to examine AD progression in a non-overlapping set of *PSEN1* carriers with available
351 clinical and biomarker measures of AD progression.

352 We found that the γ-secretase composite measure explained substantial
353 biomarker heterogeneity across *PSEN1* pathogenic mutation carriers using available
354 data from DIAN. Focusing on associations between the γ-secretase composite and Aβ
355 PET, we observed that individuals who carried pathogenic variants in the lowest (most
356 pathogenic) tertile had, on average, 1.4 SUVR units greater Aβ PET signal compared to
357 those with variants in the highest (least pathogenic) tertile, after accounting for age and
358 sex. Putting these differences in the context of the conventionally used threshold for Aβ
359 PET positivity in this cohort and with this Aβ PET tracer (cortical PiB PET SUVR positive
360 at >= 1.42 SUVR[30]), carriers of pathogenic variants in the lowest (most pathogenic)
361 tertile of the γ-secretase composite would, on average, become amyloid positive ~15
362 years sooner than those carrying *PSEN1* variants in the highest (least pathogenic)
363 tertile (estimated mean age of 22.6 and 37.2 years for low and high tertiles,
364 respectively). Consistent with cross-sectional results, analysis of longitudinal data
365 demonstrated that Aβ PET signal increased more quickly in individuals carrying *PSEN1*
366 variants with lower (more pathogenic) γ-secretase composite scores compared to those
367 with higher composite scores. Though further work is needed to elucidate regional
368 differences, the results here also suggest that variants with low γ-secretase composite

369 values may have greater striatal Aβ PET signal compared to carriers of *PSEN1* variants
370 with high composite values.

371 Cerebrospinal fluid measures of AD pathology also had significant associations
372 with the variant-level γ-secretase composite, including CSF measures of Aβ42/40 and
373 phosphorylated-tau181, and phosphorylated-tau217. In addition to associations with
374 core measures of AD pathobiology, γ-secretase composite scores correlated with FDG
375 PET and structural MRI, two commonly used neuroimaging measures of
376 neurodegeneration. Together with the described associations with AAO and functional
377 impairment measures, this broad pattern of association between γ-secretase function
378 with core AD and neurodegenerative markers further support the hypothesis that
379 heterogeneity in ADAD can broadly be understood in the context of mutation-level
380 differences in γ-secretase dysfunction. Importantly, despite variations in AAO and
381 biomarker trajectories across variants, the results here also support prior observations
382 that pathologic changes in Aβ and tau consistently precede neurodegenerative changes
383 and clinical impairment across *PSEN1* variants[25,26,37]. Additionally, as the γ-secretase
384 composite used here was derived to predict AAO, it remains quite possible that different
385 formulations of this summary measure of γ-secretase function will be better optimized to
386 predict particular biomarker trajectories in clinical trial settings.

387 The results here need to be considered in the context of certain limitations.
388 Though AAO information was available on all *PSEN1* variants examined, only a subset
389 had available clinical, cognitive, and biomarker data from the DIAN-Obs study.
390 Accordingly, data from new pathogenic variants in DIAN and in the broader scientific
391 literature will need to be considered. Similarly, tau PET data will need to be considered

392 in future analyses as they become available. Further, it will be important to determine if
393 processing of γ-secretase substrates besides APP is additionally informative for
394 understanding the differential pathogenicity across *PSEN1* variants. Lastly, it will be
395 critical to extend the cell-based model system to allow for the characterization of
396 pathogenic variants in *PSEN2* and *APP*, as ~20% of ADAD-causing variants are found
397 within these genes.

398 Despite these limitations, these findings indicate that variant level differences in
399 γ-secretase function are highly associated with core measures of clinical, biomarker,
400 and cognitive, progression of ADAD, and suggest that these variant-level differences
401 explain a large portion of the heterogeneity seen across *PSEN1* pathogenic mutation
402 carriers. As the biochemical measures of γ-secretase function used here are derived
403 outside the context of family polygenic factors, age, and estimated years to symptom
404 onset, they offer a potentially unique channel of information with respect to disease
405 progression compared to these other factors and may thus represent useful
406 complements to these measures in ADAD clinical trials. Similarly, as these cell-based
407 measures are divorced from family polygenic factors and age, they may prove to be
408 valuable in gauging the impact of genetic and lifestyle factors that may confer resilience
409 or risk for ADAD onset and progression. Cell-based measures of γ-secretase function
410 may be particularly useful to assess pathogenicity, potential AAO, and predicted AD
411 trajectories for newly discovered *PSEN1* pathogenic variants or for variants lacking
412 sufficient clinical history. Importantly, these results also strongly support the continued
413 investigation of γ-secretase modulators as an AD therapeutic strategy. Lastly, by
414 demonstrating a tight linkage between the processing of APP by γ-secretase in a cell-

415 based model system and ADAD disease trajectories *in vivo*, the results here provide
416 strong support for the hypothesis that dysregulation of APP processing is central to AD
417 pathogenesis, offing support for some formulations of the "Aβ hypothesis" of AD
418 pathogenesis.
419

420 **AUTHORS' CONFLICT OF INTERESTS**

421 Partial funding from the Alzheimer's Association (SAS), NIH grants (CRJ, GSD, JMN,
422 JCM, RJB, TLSB, JPC), NIA grants (GSD), GHR Foundation (CRJ), Alexander Family
423 Alzheimer's Disease Research Professorship of Mayo Clinic (CRJ), grants from Lilly
424 (NGR), Biogen (NGR), AbbVie (NGR, JL), Chan-Zuckerberg Initiative (GSD), DZNE
425 (JL), Eisai (CR), Instituto de Salud Carlos III (RSV), Anonymous Foundation (PRS).

426 Consultations have been declared for Humana Healthcare (JPC), Roche (NCF, JL, CR,
427 RSV, RJB), Biogen (NCF, JL, CR), Parabon Nanolabs Inc. (GSD), DynaMed (EBSCO
428 Health) (GSD), medical testimony on legal cases pertaining to management of
429 Wernicke Encephalopathy (GSD), MODAG (JL), GmbH (JL), Bayer Vital (JL), Axon
430 Neuroscience (JL), Thieme Medical Publishers (JL), Prothena (CR), Wave
431 Pharmaceuticals (RSV), Janssen (RSV), Neuraxpharm (RSV), Eisai (RJB), and Amgen
432 (RJB). Other financial interests include owning stocks greater than $10000 are held in
433 ANI Pharmaceuticals (GSD), being a member of the DIAN-TU Pharma Consortium
434 which includes funding and non-financial support for the DIAN-TU-001 trial from Avid
435 Radiopharmaceuticals, Janssen Hoffman Roche/Genentech, Eli Lilly & Co, Eisai,
436 Biogen, AbbVie, and Bristol Meyer Squibbs (RJB, TLSB), and royalties from C2N
437 Diagnostics with equity ownership interest (RJB).

Non-financial interests include serving on an independent data monitoring board for Roche (CRJ), support from Lilly (NCF), support from Ionis (NCF), serving as director of Anti- NMDA Receptor Encephalitis Foundation (GSD), Eisai (TLSB), Siemens (TLSB), and a member of speaker's bureau for Biogen (TLSB).

All other authors have nothing to disclose.

ACKNOWLEDGMENTS:

Data collection and sharing for this project was supported by the Dominantly Inherited Alzheimer Network (DIAN, U19AG032438) funded by the National Institute on Aging (NIA), the Alzheimer's Association (SG-20-690363-DIAN), the German Center for Neurodegenerative Diseases (DZNE), Raul Carrea Institute for Neurological Research (FLENI). Partial support by the Research and Development Grants for Dementia from Japan Agency for Medical Research and Development, AMED, and the Korea Health Technology R&D Project through Korea Health Industry Development Institute (KHIDI), Spanish Institute of Health Carlos III (ISCIII), Canadian Institutes of Health Research (CIHR), Canadian Consortium of Neurodegeneration and Aging, Brain Canada Foundation and Fonds de Recherche du Québec – Santé. This manuscript has been reviewed by DIAN Study investigators for scientific content and consistency of data interpretation with previous DIAN Study publications. We acknowledge the altruism of the participants and their families, and contributions of the DIAN research and support staff at each of the participating sites for their contributions to this study.

461 **REFERENCES:**

462 1. Lagomarsino VN, Pearse RV, Liu L, et al. Stem cell-derived neurons reflect features of
463 protein networks, neuropathology, and cognitive outcome of their aged human donors.
464 *Neuron*. 2021;109(21):3402-3420.e9. doi:10.1016/j.neuron.2021.08.003

465 2. Hsu S, Gordon BA, Hornbeck R, et al. Discovery and validation of autosomal dominant
466 Alzheimer's disease mutations. *Alz Res Therapy*. 2018;10(1):67. doi:10.1186/s13195-018-
467 0392-9

468 3. Karch CM, Hernández D, Wang JC, et al. Human fibroblast and stem cell resource from the
469 Dominantly Inherited Alzheimer Network. *Alzheimers Res Ther*. 2018;10(1):69.
470 doi:10.1186/s13195-018-0400-0

471 4. Lanoiselée HM, Nicolas G, Wallon D, et al. APP, PSEN1, and PSEN2 mutations in early-
472 onset Alzheimer disease: A genetic screening study of familial and sporadic cases. *PLoS*
473 *Med*. 2017;14(3):e1002270. doi:10.1371/journal.pmed.1002270

474 5. De Strooper B, Iwatsubo T, Wolfe MS. Presenilins and γ-secretase: structure, function, and
475 role in Alzheimer Disease. *Cold Spring Harb Perspect Med*. 2012;2(1):a006304.
476 doi:10.1101/cshperspect.a006304

477 6. Fernandez MA, Klutkowski JA, Freret T, Wolfe MS. Alzheimer presenilin-1 mutations
478 dramatically reduce trimming of long amyloid β-peptides (Aβ) by γ-secretase to increase 42-
479 to-40-residue Aβ. *J Biol Chem*. 2014;289(45):31043-31052. doi:10.1074/jbc.M114.581165

480 7. Liu L, Lauro BM, Wolfe MS, Selkoe DJ. Hydrophilic loop 1 of Presenilin-1 and the APP
481 GxxxG transmembrane motif regulate γ-secretase function in generating Alzheimer-causing
482 Aβ peptides. *Journal of Biological Chemistry*. 2021;296:100393.
483 doi:10.1016/j.jbc.2021.100393

484 8. Wolfe MS. Dysfunctional γ-Secretase in Familial Alzheimer's Disease. *Neurochem Res*.
485 2019;44(1):5-11. doi:10.1007/s11064-018-2511-1

486 9. Wolfe MS, Selkoe DJ. Giving Alzheimer's the old one-two. *Cell*. 2010;142(2):194-196.
487 doi:10.1016/j.cell.2010.07.006

488 10. Szaruga M, Munteanu B, Lismont S, et al. Alzheimer's-Causing Mutations Shift Aβ Length
489 by Destabilizing γ-Secretase-Aβn Interactions. *Cell*. 2017;170(3):443-456.e14.
490 doi:10.1016/j.cell.2017.07.004

491 11. Wolfe MS. Probing Mechanisms and Therapeutic Potential of γ-Secretase in Alzheimer's
492 Disease. *Molecules*. 2021;26(2):E388. doi:10.3390/molecules26020388

493 12. Nie P, Vartak A, Li YM. γ-Secretase inhibitors and modulators: Mechanistic insights into the
494 function and regulation of γ-Secretase. *Semin Cell Dev Biol*. 2020;105:43-53.
495 doi:10.1016/j.semcdb.2020.03.002

496 13. Raven F, Ward JF, Zoltowska KM, et al. Soluble Gamma-secretase Modulators Attenuate
497 Alzheimer's β-amyloid Pathology and Induce Conformational Changes in Presenilin 1.
498 *EBioMedicine*. 2017;24:93-101. doi:10.1016/j.ebiom.2017.08.028

499 14. *Psen-1| Alzforum. (n.d.). Retrieved August 09, 2021, from*
500 *Https://Www.Alzforum.Org/Mutations/Psen-1*.

501 15. Ryan NS, Nicholas JM, Weston PSJ, et al. Clinical phenotype and genetic associations in
502 autosomal dominant familial Alzheimer's disease: a case series. *The Lancet Neurology*.
503 2016;15(13):1326-1335. doi:10.1016/S1474-4422(16)30193-4

504 16. Ryman DC, Acosta-Baena N, Aisen PS, et al. Symptom onset in autosomal dominant
505 Alzheimer disease: a systematic review and meta-analysis. *Neurology*. 2014;83(3):253-260.

506 17. Lippa CF, Swearer JM, Kane KJ, et al. Familial Alzheimer's disease: site of mutation
507 influences clinical phenotype. *Ann Neurol*. 2000;48(3):376-379.

508 18. Wegiel J, Wisniewski HM, Kuchna I, et al. Cell-Type-Specific Enhancement of Amyloid-β
509 Deposition in a Novel Presenilin-1 Mutation (P117L): *Journal of Neuropathology and*
510 *Experimental Neurology*. 1998;57(9):831-838. doi:10.1097/00005072-199809000-00004

511 19. Klunk WE, Price JC, Mathis CA, et al. Amyloid Deposition Begins in the Striatum of
512 Presenilin-1 Mutation Carriers from Two Unrelated Pedigrees. *Journal of Neuroscience*.
513 2007;27(23):6174-6184. doi:10.1523/JNEUROSCI.0730-07.2007

514 20. Tang M, Ryman DC, McDade E, et al. Neurological manifestations of autosomal dominant
515 familial Alzheimer's disease: a comparison of the published literature with the Dominantly
516 Inherited Alzheimer Network observational study (DIAN-OBS). *The Lancet Neurology*.
517 2016;15(13):1317-1325.

518 21. Ryan NS, Rossor MN. Correlating familial Alzheimer's disease gene mutations with clinical
519 phenotype. *Biomarkers Med*. 2010;4(1):99-112. doi:10.2217/bmm.09.92

520 22. Chhatwal JP, Schultz SA, McDade E, et al. Variant-dependent heterogeneity in amyloid β
521 burden in autosomal dominant Alzheimer's disease: cross-sectional and longitudinal
522 analyses of an observational study. *Lancet Neurol*. 2022;21(2):140-152. doi:10.1016/S1474-
523 4422(21)00375-6

524 23. Kumar-Singh S, Theuns J, Van Broeck B, et al. Mean age-of-onset of familial alzheimer
525 disease caused by presenilin mutations correlates with both increased Aβ42 and decreased
526 Aβ40. *Hum Mutat*. 2006;27(7):686-695. doi:10.1002/humu.20336

527 24. Szaruga M, Veugelen S, Benurwar M, et al. Qualitative changes in human γ-secretase
528 underlie familial Alzheimer's disease. *J Exp Med*. 2015;212(12):2003-2013.
529 doi:10.1084/jem.20150892

530 25. Liu L, Lauro BM, He A, et al. Identification of the Aβ37/42 peptide ratio in CSF as an
531 improved Aβ biomarker for Alzheimer's disease. *Alzheimers Dement*. Published online
532 March 12, 2022. doi:10.1002/alz.12646

533 26. Petit D, Fernández SG, Zoltowska KM, et al. Aβ profiles generated by Alzheimer's disease
534 causing PSEN1 variants determine the pathogenicity of the mutation and predict age at
535 disease onset. *Mol Psychiatry*. 2022;27(6):2821-2832. doi:10.1038/s41380-022-01518-6

536 27. Bateman RJ, Xiong C, Benzinger TLS, et al. Clinical and Biomarker Changes in Dominantly
537 Inherited Alzheimer's Disease. *New England Journal of Medicine*. 2012;367(9):795-804.
538 doi:10.1056/NEJMoa1202753

539 28. Wechsler D. Wechsler Memory Scale (3rd ed.): Administration and scoring manual.
540 Published online 1997.

541 29. Barthélemy NR, Li Y, Joseph-Mathurin N, et al. A soluble phosphorylated tau signature
542 links tau, amyloid and the evolution of stages of dominantly inherited Alzheimer's disease.
543 *Nat Med*. 2020;26(3):398-407. doi:10.1038/s41591-020-0781-z

544 30. Su Y, D'Angelo GM, Vlassenko AG, et al. Quantitative Analysis of PiB-PET with
545 FreeSurfer ROIs. *PLOS ONE*. 2013;8(11):e73377. doi:10.1371/journal.pone.0073377

546 31. Su Y, Blazey TM, Owen CJ, et al. Quantitative Amyloid Imaging in Autosomal Dominant
547 Alzheimer's Disease: Results from the DIAN Study Group. *PLoS One*.
548 2016;11(3):e0152082. doi:10.1371/journal.pone.0152082

549 32. Gordon BA, Blazey TM, Su Y, et al. Spatial patterns of neuroimaging biomarker change in
550 individuals from families with autosomal dominant Alzheimer's disease: a longitudinal
551 study. *The Lancet Neurology*. 2018;17(3):241-250.

552 33. McKay NS, Gordon BA, Hornbeck RC, et al. *Neuroimaging within the Dominantly Inherited*
553 *Alzheimer's Network (DIAN): PET and MRI*. Neuroscience; 2022.
554 doi:10.1101/2022.03.25.485799

555 34. Gu L, Guo Z. Alzheimer's Aβ42 and Aβ40 peptides form interlaced amyloid fibrils. *J*
556 *Neurochem*. 2013;126(3):305-311. doi:10.1111/jnc.12202

557 35. Cullen N, Janelidze S, Palmqvist S, et al. Association of CSF Aβ38 Levels With Risk of
558 Alzheimer Disease-Related Decline. *Neurology*. 2022;98(9):e958-e967.
559 doi:10.1212/WNL.0000000000013228

560 36. Toyn JH, Boy KM, Raybon J, et al. Robust Translation of -Secretase Modulator
561 Pharmacology across Preclinical Species and Human Subjects. *Journal of Pharmacology*
562 *and Experimental Therapeutics*. 2016;358(1):125-137. doi:10.1124/jpet.116.232249

563 37. Sun L, Zhou R, Yang G, Shi Y. Analysis of 138 pathogenic mutations in presenilin-1 on the
564 in vitro production of Aβ42 and Aβ40 peptides by γ-secretase. *Proc Natl Acad Sci U S A*.
565 2017;114(4):E476-E485. doi:10.1073/pnas.1618657114

TABLES AND FIGURES

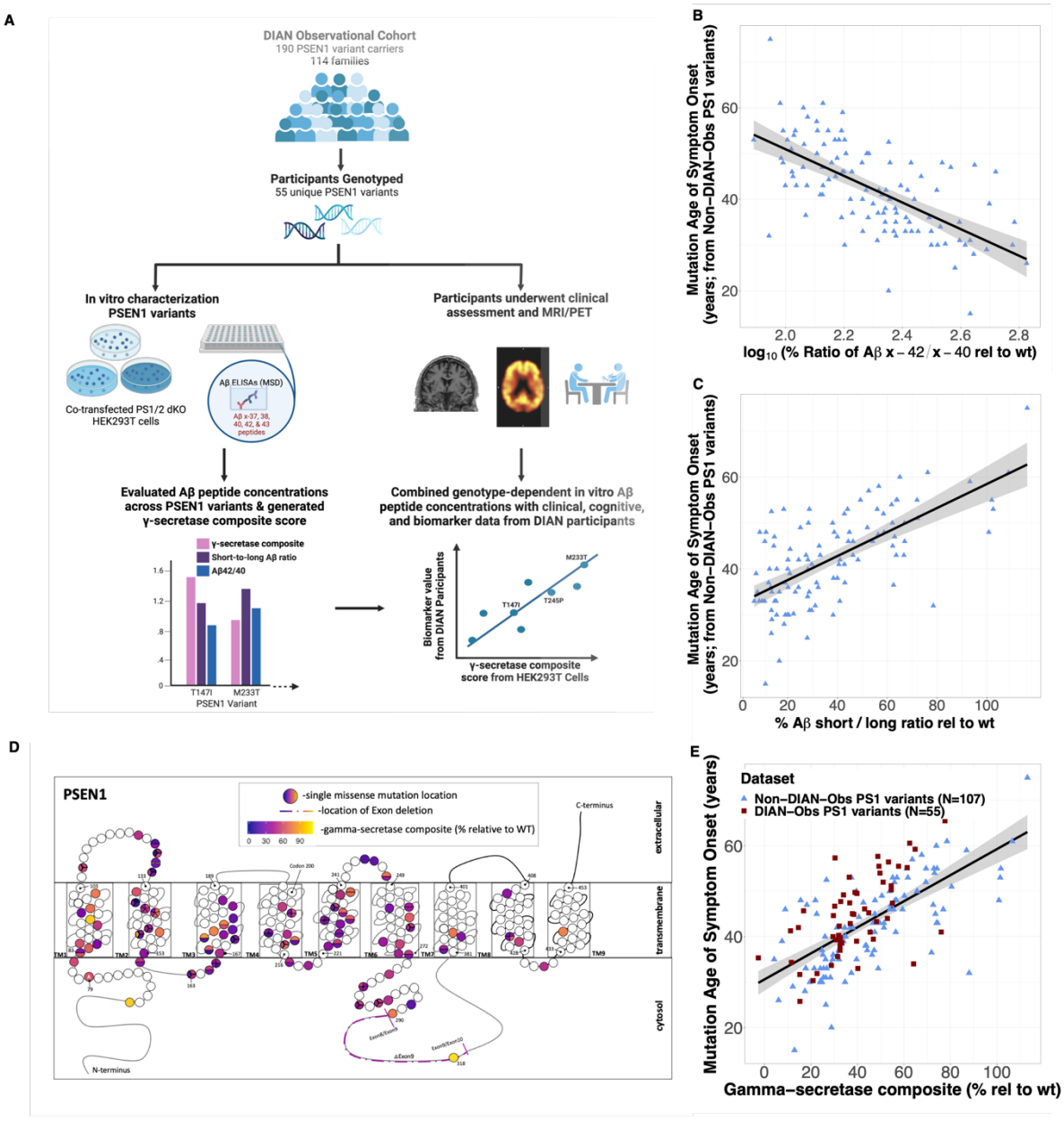

Figure 1. Cell-based measures of γ-secretase function are tightly associated with age of symptom onset across two cohorts representing 161 unique *PSEN1* variants. (A) Schematic summarizing the characterization of variant-level γ-secretase function and correlations with age of symptom onset, cognitive, and biomarker data for each variant (created with BioRender.com). γ-secretase function was summarized using

574 two ratios of Aβ peptide production derived from cell models (**B**) Cell-based $\log_{10}(\frac{A\beta 42}{A\beta 40})$

575 levels and (**C**) a ratio of short (fully γ-secretase processed) to long (incompletely γ-

576 secretase processed) Aβ fragments ($\frac{\text{short } A\beta 37+38}{\text{long } A\beta 42+43}$) . Both ratios were independently

577 associated with age of symptom onset in an initial set of 106 *PSEN1* variants (B-C). To

578 reduce comparisons going forward, both ratios were combined into a single composite

579 measure (γ-secretase composite, expressed as a percentage of normal γ-secretase

580 function; D). This composite measure correlated with age of symptom onset in both the

581 initial set of 106 *PSEN1* variants and in a second set of 55 *PSEN1* variants represented

582 in DIAN-Obs (E). Individual data points are jittered to maintain blinding.

583

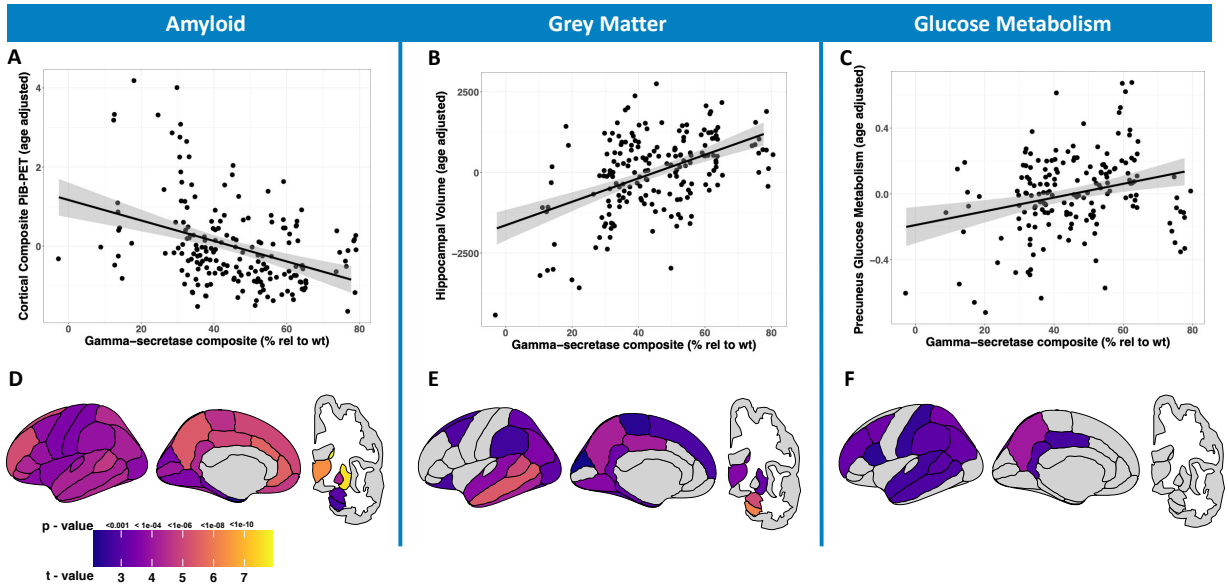

Figure 2. Lower γ-secretase function across variants is associated with more abnormal AD imaging biomarkers. Association between variant-level γ-secretase function and in *vivo* imaging biomarker data from carriers of corresponding *PSEN1* pathogenic variants is shown for cross-sectional Aβ PET (age-adjusted PiB-PET SUVR cortical composite, **A**), age- and intracranial volume-adjusted bilateral hippocampal grey matter volume derived from structural MRI (**B**), and age-adjusted bilateral precuneus FDG-PET SUVR (**C**) from 190 *PSEN1* pathogenic variant carriers (55 unique variants represented). Individual data points are jittered to maintain blinding of the data. Exploratory, regional analyses comparing PiB-PET SUVRs (**D**), grey matter volumes (**E**), and FDG-PET SUVRs (**F**) across a range of γ-secretase function, with colors indicating t- and p-values derived from the comparison of neuroimaging data from *PSEN1* carriers with variants in the lowest (most pathogenic) vs. highest (least pathogenic) tertiles of γ-secretase composite function. Models additionally adjusted for age and sex. Individual data points are jittered to maintain blinding.

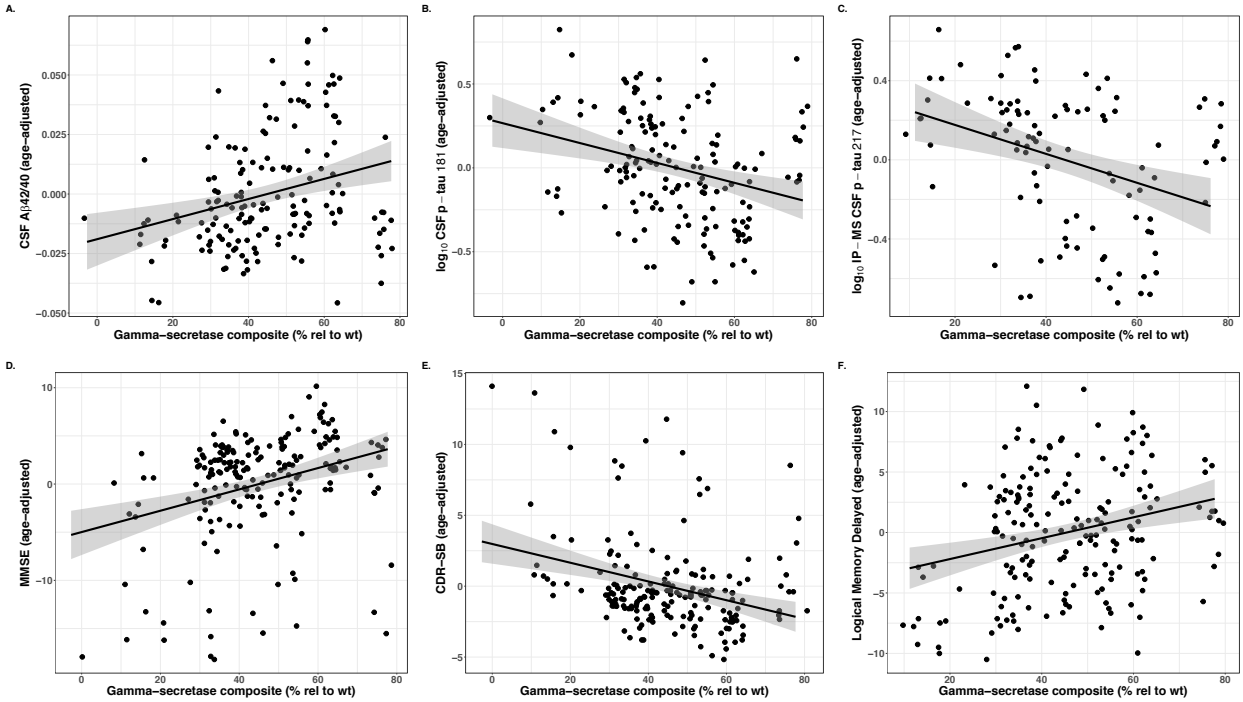

Figure 3. Lower γ-secretase function across variants is associated with more abnormal biofluid, clinical, and cognitive measures in ADAD. Associations between γ-secretase function for each *PSEN1* variant and cross-sectional CSF Aβ 42/40 (**A**), age-adjusted CSF $\log_{10}$ pT181 (**B**), CSF $\log_{10}$ pT217/T217 (**C**), age-adjusted MMSE (**D**), age-adjusted CDR-SB (**E**), and age-adjusted logical memory-delayed (**F**) values from 190 *PSEN1* pathogenic variant carriers (55 unique variants represented) are shown. Individual data points are jittered to maintain blinding.

CSF = Cerebrospinal Fluid; pT = phosphorylated tau; MMSE = Mini Mental State Examination scores; CDR-SB = Clinical Dementia Rating Scale- Sum of Boxes.

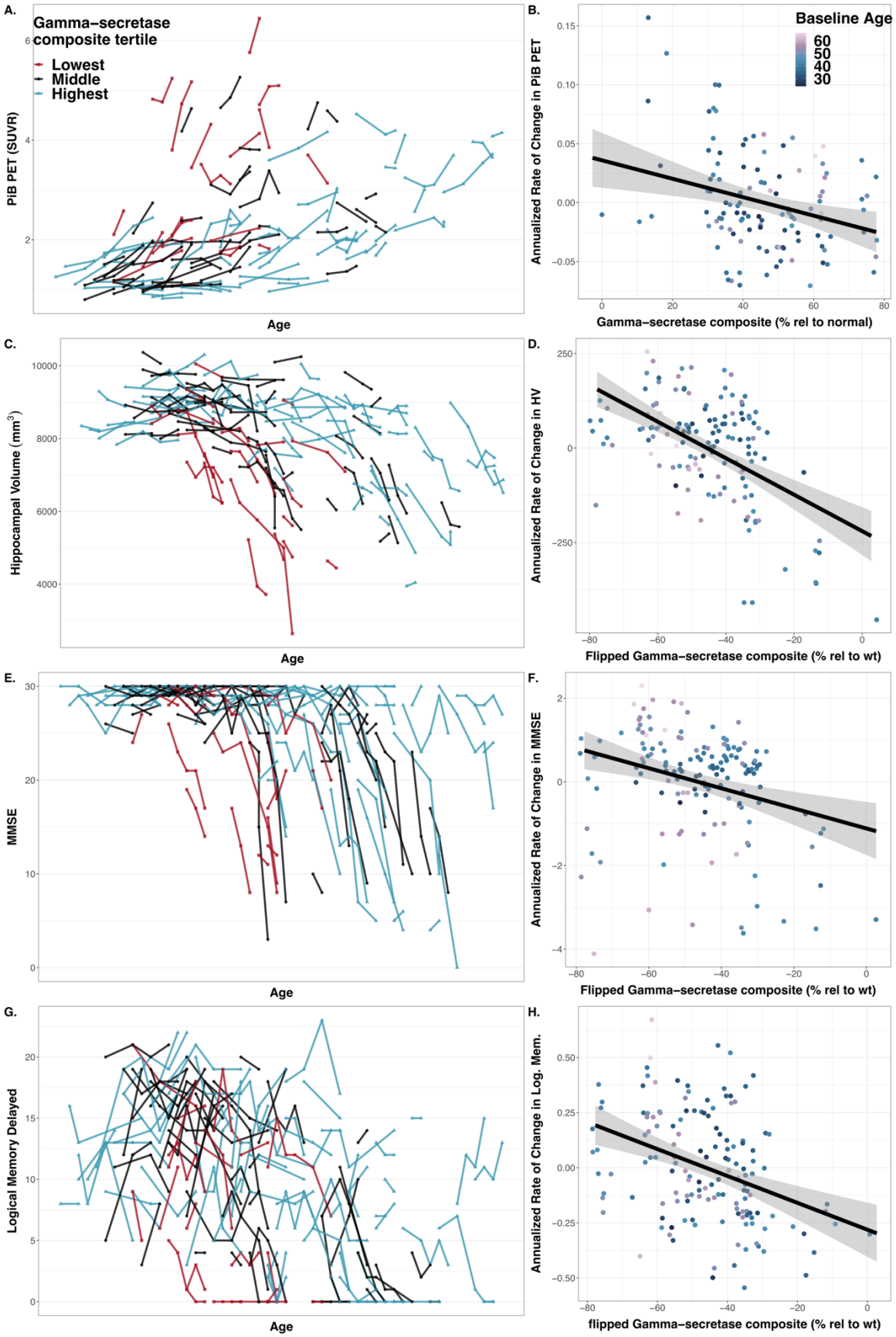
A.
Gamma−secretase composite tertile
Lowest
Middle
Highest
PiB PET (SUVR)
Age
B.
Baseline Age
60
50
40
30
Annualized Rate of Change in PiB PET
Gamma−secretase composite (% rel to normal)
C.
Hippocampal Volume (mm3)
Age
D.
Annualized Rate of Change in HV
Flipped Gamma−secretase composite (% rel to wt)
E.
MMSE
Age
F.
Annualized Rate of Change in MMSE
Flipped Gamma−secretase composite (% rel to wt)
G.
Logical Memory Delayed
Age
H.
Annualized Rate of Change in Log. Mem.
flipped Gamma−secretase composite (% rel to wt)

611

612 **Figure 4. Lower γ-secretase function across *PSEN1* variants is associated with**
613 **more rapid worsening in biomarker, clinical and cognitive measures in ADAD.**
614 Individual longitudinal measures are plotted for PiB-PET SUVR (Aβ burden; **A**),
615 hippocampal volume (HV; mm^3; **C**), Mini Mental Status Exam (MMSE; **E**), and logical
616 memory delayed (Log. Mem.; **G**). Colors indicate whether an individual's *PSEN1* variant
617 is in the low (red; most pathogenic tertile), middle (black; intermediate pathogenicity), or
618 high (blue; least pathogenic) tertile for γ-secretase function. To facilitate statistical
619 comparison, age-adjusted, individual-level slopes for each biomarker and cognitive
620 outcomes of interest were extracted from linear mixed effects models and plotted
621 against γ-secretase function (Aβ PET – **B**; Hippocampal Volume – **D**; MMSE – **F**;
622 Logical Memory – **H**). Significant associations were observed between rate-of-change
623 in each measure and variant-level γ-secretase function. Individual data points are
624 jittered to maintain blinding.
625

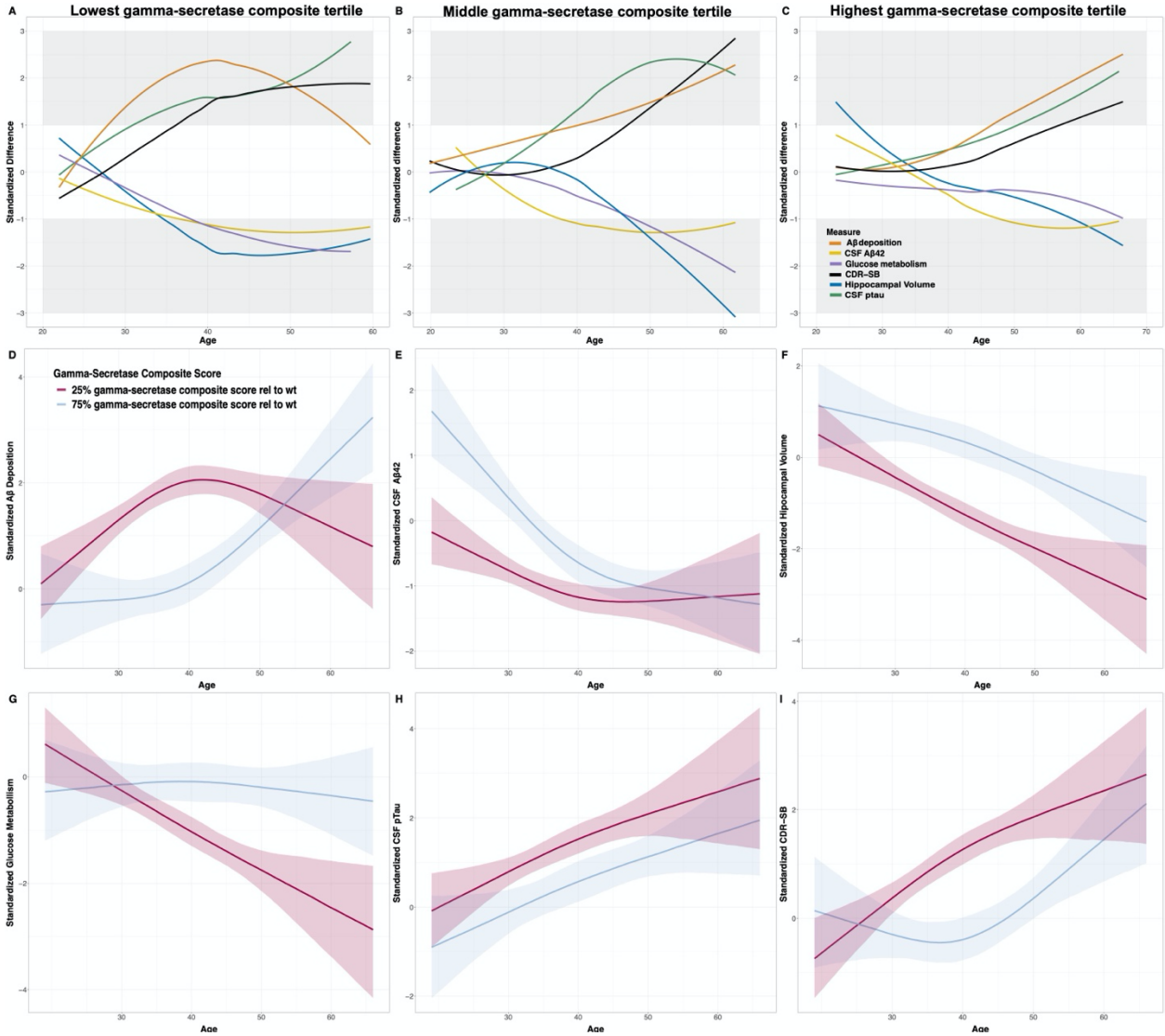

Figure 5. Variant-level variations in γ-secretase function are broadly associated with the clinical and biomarker course of ADAD and can be used to predict ADAD progression for novel *PSEN1* pathogenic variants. To visualize how variant-level differences in γ-secretase function may broadly alter the clinical, cognitive, and biomarker course of ADAD, we plotted the standardized differences in core clinical, cognitive, and biomarker measures across the lifespan for DIAN-Obs participants carrying *PSEN1* pathogenic variants in the lowest (**A**), middle (**B**), or highest (**C**) tertile of γ-secretase function compared to non-carriers. This group-level analysis was followed

635 by an individual-level visualization of disease trajectories for pathogenic variant carriers

636 of 2 possible variants with 25% and 75% of normal γ-secretase function, respectively

637 (D-I).